ACS APPLIED MATERIALS & INTERFACES

Research Article

www.acsami.org

Heteroaggregation between PEI-Coated Magnetic Nanoparticles and Algae: Effect of Particle Size on Algal Harvesting Efficiency

Shijian Ge, Michael Agbakpe, Wen Zhang,* and Liyuan Kuang

John A. Reif, Jr. Department of Civil and Environmental Engineering, New Jersey Institute of Technology, Newark, New Jersey 07102, United States

Supporting Information

ABSTRACT: Colloidal interactions between magnetic nanoparticles (NPs) and algal cells are of paramount significance to magnetophoretic separation of algal biomass from water. This study evaluated the size effect of magnetic NPs (MNPs) coated with polyethylenimine (PEI) on the separation efficiency of *Scenedesmus dimorphus* as well as on the recovery efficiency of MNPs from algal biomass. Results showed that algal harvesting efficiency (HE) increased from ca. 60% to 85% as the diameter of PEI-coated MNPs increased from 9 to 53 nm. Likewise, algal recovery capacity (algae/MNPs, w/w) also showed the same size dependence. But a large size (247 nm) led to a decline of algal HE, which was correctly interpreted by a settling model that predicts large sizes of MNPs could eventually reduce the settling velocity under magnetophoresis. The extended Derjaguin−Landau−Verwey−Overbeek theory revealed that the particle size and PEI coating both influenced the interaction energies (e.g., energy barrier) between MNPs and algae. Particularly, PEI coating significantly reduced the energy barrier between MNPs and algae and thereby increased their heteroaggregation and algal HE. Moreover, PEI-coated MNPs were recovered from the harvested algae biomass through a chemical-free ultrasonic method, and the recovery efficiency appeared to be higher for larger MNPs. Overall, the synthesized sizes of applied MNPs will not only affect algal HE but also have economic implications on magnetophoretic algal separation technologies.

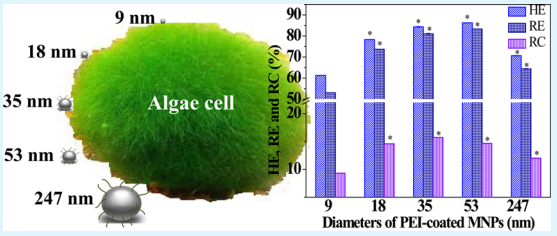

KEYWORDS: *magnetic nanoparticles, magnetophoretic separation, algae, biofuel, harvesting, EDLVO*

INTRODUCTION

The harvesting and dewatering of algae biomass from large-volume liquid culture medium remains one of several significant processing bottlenecks for industrialization of algae-derived biofuels.[1−3] Despite extensive research on harvesting methods, the majority (e.g., coagulation, filtration, or centrifugation) of methods are not sufficiently cost-effective.[3] Magnetophoretic separation has been regarded among the efficient methods for algal biomass recovery or removal from water.[4−7] This separation process operates by tagging nonmagnetic algal cells with magnetic particles to increase magnetic susceptibility between algae and the culture medium.[5] Under the external magnetic field, the magnetically modified algal cells are rapidly concentrated into compact slurry that is separated from the bulk liquid in a short time (usually a few minutes; see a summary in Table S1 in Supporting Information).[6] Besides the high algal separation efficiency, magnetophoretic separation technology offers several other unique advantages:[8] (1) low operational cost and energy consumption; (2) flexible implementation (point-of-service); and (3) potential to recover and reuse magnetic particles,[9] thereby increasing sustainability and economic viability of algal biofuel production. Because of the low fabrication cost, enhanced surface areas, and tunable physicochemical properties, magnetite (Fe_3O_4) nanoparticles (NPs) are commonly used as the paramagnetic core materials.[7,9] To increase interactions with negatively charged algal cells, magnetite particles are often coated with cationic polymers such as poly(diallyldimethylammonium chloride) (PDDA),[10,11] polyethlenimine (PEI),[12] or natural cationic biopolymers (e.g., chitosan).[13] Besides magnetite, other magnetic materials such as aminoclay−nanoscale zerovalent iron (nZVI) composites were also reported in the algal separation.[14]

Colloidal surface interactions are the first step for the heteroaggregation between algal cells and magnetic particles, which is crucial for the success of magnetophoretic separation. According to the extended Derjaguin−Landau−Verwey−Overbeek (EDLVO) theory,[15,16] the surface interactions between algae and magnetic particles are likely mediated by at least three colloidal forces, namely, van der Waals attraction, electrostatic attraction, and steric force due to the presence of biopolymers and polymer coatings on algae and magnetic particles, respectively. The complex interplay of the aforementioned interaction forces plays a profound role in the particle−algae heteroaggregation. Generally, both physical or chemical properties of the interacting surfaces and the electrolytic environment (e.g., ionic strength and pH) can significantly influence the aforementioned colloidal forces.[17,18] For example,

Received: November 24, 2014
Accepted: March 4, 2015
Published: March 4, 2015

DOI: 10.1021/acsami.5b00572
ACS Appl. Mater. Interfaces 2015, 7, 6102−6108

many studies indicated that surface charge influences the electrostatic interactions between algae and NPs (e.g., Ag, TiO_2, or ZnO).[19−21] Moreover, the particle size also likely affects heteroaggregation between magnetic NPs (MNPs) and algae,[22] which has not been reported. In particular, magnetite nanostructures differ substantially from its bulk phase counterpart and exhibit size-dependent properties (specific surface area, surface reactivity, and magnetic response).[23−25] Clearly, changes to magnetic particle properties could greatly affect colloidal interactions with algae, thereby algal harvesting efficiency (HE) as well as the optimal dose demand for MNPs. In addition, particle size could also affect the detachment of magnetic NPs from algae, which might be important for recovering and reusing MNPs. A low dose demand with particle reuse in magnetophoretic separation is highly desirable as it is expected to have a lower potential to contaminate algae biomass and a lower operational cost.

This work aims to evaluate the primary size effect of MNPs on algae interactions and algal HE. Differently sized magnetite NPs coated with PEI were synthesized by the coprecipitation method. Magnetic algal separation efficiencies with these MNPs were compared. The EDLVO theory was used to interpret the size effects on the colloidal interaction energy between uncoated or PEI-coated MNPs and algae. The size effects on reusability of MNPs and economic viability were also examined.

MATERIALS AND METHODS

Algae Culture. *Scenedesmus dimorphus* was cultivated in the modified Bold's Basal Medium (MBBM) in a 2 L Erlenmeyer flask at room temperature (25 ± 1 °C) with 5% CO_2 at a rate of 8.5×10^{-4} liters of CO_2·per minute·(per liter of medium) $^{-1}$.[26,27] The light−dark cycle (12 h/12 h) was maintained at a photon flux of ∼1200 lx (27.4 μmol·m^{-2}·s^{-1} or 4200 mW·m^{-2}) measured by a spectroradiometer (Spectral Evolution, SR-1100).[28] The algal concentration (g·L^{-1}) was characterized by the dry cell weight (DCW). The initial inoculated algal concentration was ∼0.2 g·L^{-1}, while the final steady-state algal concentration after 14 d of incubation was ∼1.8 g·L^{-1}.

Preparation and Characterization of Polyethylenimine-Coated Magnetic Nanoparticles. MNPs with primary particle diameters of 9 and 18 nm were prepared using the chemical coprecipitation methods.[9] Briefly, 0.99 g of $FeCl_2$·$4H_2O$ and 2.7 g of $FeCl_3$·$6H_2O$ were dissolved in a flask vessel containing 100 mL of deoxygenated deionized (DI) water with vigorous stirring under nitrogen atmosphere at 80 °C, and then 10 mL of NH_4OH (25 wt %) was added into the above solution. The mixture was stirred continuously for 30 min, and the color of the solution changed gradually from light brown to black. The resulting magnetite was separated from the mixture using a NdFeB permanent block magnet (K&J Magnetics, Inc., Pipersville, PA) and washed four times with DI water. The synthesized MNPs were ∼9 nm in diameter and were stored in DI water for further use. The 18 nm MNPs were synthesized in the same fashion as stated above except that the synthesized 9 nm MNPs were added as the growth nuclei (seed) to produce 18 nm MNPs.[29] The larger sized MNPs (35, 53, and 247 nm) were synthesized using the oxidation precipitation method.[30] Under a given molar ratio of $Fe^{2+}/NO_3^-/OH^-$ = 3:1:5, the $FeCl_2$ solution (0.1 or 0.5 M) was slowly added into the NaOH solution (0.02 or 0.5 M) under stirring. After running out of the $FeCl_2$ solution for 5 min, a calculated amount of $NaNO_3$ solution (0.5 M) was added slowly into the $FeCl_2$−NaOH solution, which was further stirred for 10 min, and then aged at 60 °C for 4 or 10 h. All the solutions used were dissolved in DI water. To coat MNPs with PEI (Mw ≈ 25 000 g·mol^{-1}, Fisher Scientific, U.S.), the water suspension of MNPs was first agitated using a sonicator (Sonic dismembrator 500, Fisher Scientific, U.S.) in a water−ice bath at 500 W and 20 kHz for 10 min. Then, PEI was added into the suspension at a mass ratio of 0.4PEI/MNPs (w/w).[31] The mixture was incubated in the room temperature on a rotatary shaker for 20 min, followed by centrifugation at 5000*g* for 10 min and rigorous washing with DI water to remove loosely attached or the suspended PEI in the solution. The collected PEI-coated MNPs were stored in DI water; prior to use, the supension was agitated by sonication.

Characterization of Magnetic Nanoparticles. The morphology and sizes of PEI-coated MNPs were determined by a Hitachi H-7500 transmission electron microscope (TEM). Moreover, zeta potentials, averaged hydrodynamic diameters, and particle size distribution (PSD) in water suspension were characterized by a dynamic light scattering (DLS) on a Zetasizer nano ZS instrument (Malvern Instruments, U.K.). Refractive indices of 2.42 and 1.23 were used, respectively, for MNPs and *S. dimorphus* cells for calculating the scattering wave vector. The contact angle (θ) for uncoated or PEI-coated MNPs was measured by the sessile drop technique using the CAM 200 goniometer (KSV Instruments, Finland). The UV−vis absorption spectra were obtained using a Thermoscientific Evolution 201PC spectrophotometer. Other characterization (e.g., XRD) was reported in our previous work.[31]

Algae Separation with Differently Sized Polyethylenimine-Coated Magnetic Nanoparticles. After 14 d of cultivation, the algal suspension in the culture medium was directly used in the magnetophoretic separation experiments. The five differently sized PEI-coated MNPs were directly applied to the suspension of *S. dimorphus* in a 25 mL glass specimen bottle at different mass loadings (0.0375:1 to 0.375:1 MNPs/algae, w/w) with the initial algal concentration of 0.8 g·L^{-1}. After rigorous mixing for 2.0 min,[7] a NdFeB permanent magnet (K&J Magnetics, Inc.) was placed under the bottle for 3.0 min to separate the algae−MNPs aggregates as illustrated in Supporting Information, Figure S1. The maximum surface magnetic field was 0.175 T as measured by a magnetometer (PS-2112, PASCO).

Three indicators, namely, algal harvesting efficiency (HE), recovery efficiency (RE), and recovery capacity (RC), were used to evaluate the algal separation performance.[9,32]

$$\mathrm{HE}(\%) = [1 - (C_t/C_0)] \times 100 \tag{1}$$

$$\mathrm{RE}(\%) = \left[1 - \left(\frac{C_t/C_0}{C_t'/C_0'}\right)\right] \times 100 \tag{2}$$

$$\mathrm{RC}(\mathrm{g-algae{\cdot}g-MNPs^{-1}}) = \frac{(C_0 - C_t)V}{m} \tag{3}$$

where C_0 and C_t are the algal concentration in the supernatant before and after separation (g·L^{-1}), C_0' and C_t' are the algal concentration without addition of MNPs in the control group (g·L^{-1}), V is the volume (20 mL) of algal suspension, and m is the mass of MNPs added (g). To measure the algal concentrations in the supernatant, liquid samples were taken from 1 cm below the surface of the algal suspension for the optical absorbance measurement at 680 nm by Thermoscientific Evolution 201PC UV−vis spectrophotometer. The MNPs concentration were represented by the total iron (Fe) concentration determined by Agilent 7500i Benchtop Inductively Coupled Plasma-Mass Spectrometer System (ICP-MS).

Effect of Particle Size on the Recovery and Reuse of Magnetic Nanoparticles. The recovery of MNPs from algae−MNPs slurry was usually achieved by adding strong acid or base to the mixture.[4,6,7] Here we presented a chemical-free approach using sonication to separate MNPs from algae biomass. The separated algae−MNPs aggregates (1.2−1.6 g of algae·per liter; 10 mL) was first agitated in the ice bath for 5 min using the sonicator at 500 W. The aggregates were then placed on top of the magnet and stirred gently for 2−3 min to facilitate the detachment of MNPs from the aggregates. Algal biomass in the upper fluid was discarded, while the detached MNPs were attracted at the container bottom by the magnet. The collected MNPs were then washed at least three times with DI water, followed by the same PEI coating process prior to the reuse in algal harvesting. The collected MNPs were quantified by ICP-MS with

DOI: 10.1021/acsami.5b00572
ACS Appl. Mater. Interfaces 2015, 7, 6102−6108

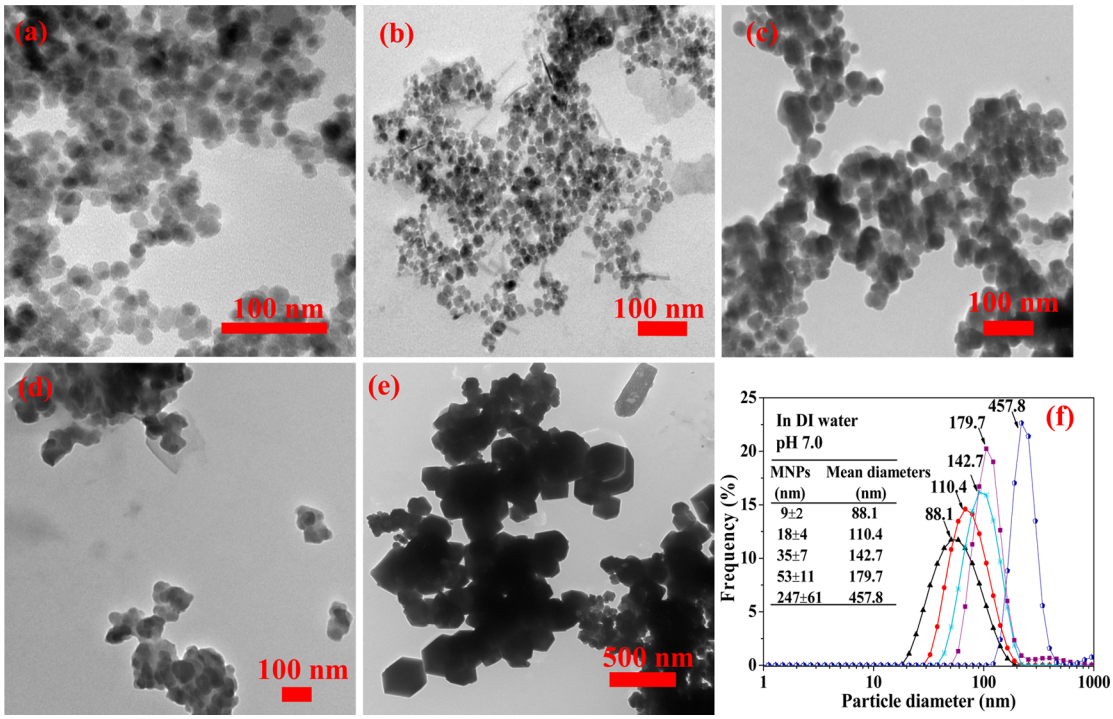

Figure 1. (a–e) TEM images of 9-, 18-, 35-, 53- and 247 nm PEI-coated MNPs. (f) Hydrodynamic PSD for five different sizes of PEI-coated MNPs in the algal medium. The table inset shows the comparison of TEM diameters (left column) and mean hydrodynamic diameters (right column) measured by DLS.

Table 1. Zeta Potentials (mV) of MNPs and *S. dimorphus* Cells in Algal Medium at pH = 7.0 ± 0.3[a]

MNPs	9 nm	18 nm	35 nm	53 nm	247 nm	*S. dimorphus*
uncoated	−21.3 ± 1.2	−21.2 ± 1.2	−23.3 ± 1.0	−20.9 ± 1.0	−25.7 ± 4.1	−29.0 ± 1.3
PEI-coated	33.8 ± 1.0	38.4 ± 1.1	19.0 ± 1.0	21.0 ± 1.7	18.7 ± 1.5	

[a]The culture medium contains the major ions of Na^+, K^+, Mg^{2+}, Ca^{2+}, Fe^{2+}, Zn^{2+}, Mn^{2+}, Cu^{2+}, Co^{2+}, H^+, NO_3^-, $H_2PO_4^-$, HPO_4^{2-}, SO_4^{2-}, Cl^-, OH^-, and MoO_4^{2-} with the ionic strength of 12.6 mM.

respect to the Fe concentration. The RE of MNPs was assessed by eq 4

$$\mathrm{RE}(\%) = \frac{V_0 \cdot C_{\mathrm{Fe},0} - V_t \cdot C_{\mathrm{Fe},t}}{V_0 \cdot C_{\mathrm{Fe},0}} \times 100 \quad (4)$$

where V_0 is the volume of the MNPs suspension initially applied to the algal suspension, V_t is the volume of the collected MNPs suspension by sonication and magnetic separation, and $C_{\mathrm{Fe},0}$ and $C_{\mathrm{Fe},t}$ are the concentrations of Fe corresponding to the above two suspension, respectively.

Comparison of Colloidal Interaction Analysis. The EDLVO theory was used to compute the interaction energies between five differently sized uncoated or PEI-coated MNPs and algae and between MNPs themselves. The van der Waals attraction, electrostatic repulsion,[33,34] magnetic forces,[35] and steric and bridging forces contributed by adsorbed PEI polymer chains[36] were all considered. The relevant equations for computing the total interaction energies are provided in details in Supporting Information, Sections S3 and S4.

Statistical Analysis. All experiments were performed at room temperature of 25 ± 3 °C with triplicate sampling and testing. The presented results are mean values ± standard deviation from three independent experiments. The differences in HE, RE, and RC values between test groups were tested for significance using one-way analysis of variance at a significant level of 0.05.

RESULTS AND DISCUSSION

Characterization. TEM images in Figure 1a–e show the morphology (spherical in shape) and clear faceted surfaces of the synthesized PEI-coated MNPs. Five distinct mean diameters (9, 18, 35, 53, and 247 nm) were achieved with the statistical PSD provided in Supporting Information, Figure S3. The hydrodynamic size distributions of PEI-coated MNPs in water dispersion are shown in Figure 1f. Moreover, because of the electrostatic and steric repulsion,[37,38] PEI-coated MNPs had stable dispersion without significant changes in size distribution during the storage and application in algal harvesting (data not shown). A larger hydrodynamic size distribution compared to the TEM size distribution was noted, mainly because of the difference in the measurement principles of TEM and DLS. In general, TEM images show the primary particle size of particles in dry solid form, whereas DLS measures hydrodynamic sizes of dispersed particles that may form small aggregates (e.g., doublet or triplet) in solution.[39−41] Also, the hydrodynamic sizes may include the thickness of polymer coating and electric double layer (EDL) surrounding the particles.[42−44] Polydispersivity indexes (PDIs) for the five different sizes of MNPs were all less than 0.25, indicating that PEI-coated MNPs did not undergo significant aggregation or sedimentation in water suspension.[22,45]

S. dimorphus algae had a negative zeta potential of ca. −29.0 ± 1.3 mV in the algal medium (Table 1).[28,31] Moreover, all sized uncoated MNPs carried negative charges, while the PEI-coated MNPs were positively charged, which resulted in the electrostatic attraction between PEI-coated MNPs and algae.

DOI: 10.1021/acsami.5b00572
ACS Appl. Mater. Interfaces 2015, 7, 6102−6108

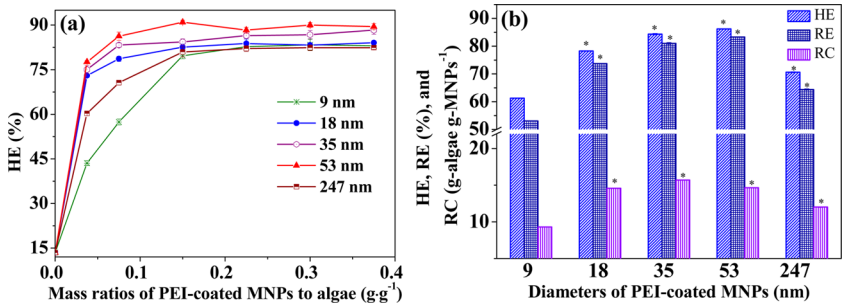

Figure 2. (a) HE (%) of *S. dimorphus* as a function of the mass ratio of PEI-coated MNPs to algae. (b) Comparisons of HE, RE (%), and RC (algae/MNPs, w/w) of *S. dimorphus* mixed with five size-dependent PEI-coated MNPs. All five differently sized MNPs were applied at a dose of 0.075 g·g^{-1} with the initial algal concentration of 0.8 g·L^{-1}. *denotes significant differences ($p < 0.05$) between the values of RE, RC, and HE for 9 nm MNPs and those for the other four sizes. The magnetic field strength is 0.099 ± 0.009 T. The solution pH, dissolved oxygen, and oxidation−reduction potential of the culture medium were 7.0 ± 1.1, 18 ± 2 mg·L^{-1}, and 170 ± 31 mV, respectively.

Algal Separation Using Differently Sized Polyethylenimine-Coated Magnetic Nanoparticles. Figure 2a shows the algal HE for five differently sized PEI-coated MNPs applied to algal suspension at different mass ratios (PEI-coated MNPs/algae, w/w). Generally, HE increased with the increase of the applied MNP dose. The maximum HE of 83−91% was achieved when MNPs reached or exceeded certain doses for different sizes of MNPs (e.g., 0.15 g·g^{-1} for 9 and 247 nm, 0.075 g·g^{-1} for the other three sizes). Compared to uncoated MNPs, algal HE substantially increased as indicated by HE or RC (Supporting Information, Table S1). Also, algal HEs using different MNPs in recent studies were summarized.[5,9,12] In comparison with naked and silica-coated MNPs,[7,9,46,47] the PEI-coated MNPs (especially large sizes) improved algal harvesting as indicated by RC/T (algae/MNPs·min^{-1}).[12]

Algal HE and dose demand for MNPs clearly show strong dependence on the primary particle size of MNPs. Figure 2b further compares the obtained HE, RE, and RC values when the five differently sized PEI-coated MNPs were applied at the same dose (0.075 g·g^{-1}). All the three harvesting indicators increased with the increase of the particle size initially when MNPs were smaller than 53 nm. A large size of MNPs (247 nm), however, decreased the HE compared to the smaller sizes of MNPs. A recent study also reported a similar finding that a greater dose was required to separate oleaginous *Chlorella sp.* for the larger barium ferrite magnetic particles.[4] Supporting Information, Table S5 shows the results of *t*-test performed to compare the differences between the data of HE, RE, and RC using differently sized MNPs. Only the RC data for 18 and 53 nm MNPs were not significantly different ($p > 0.05$), whereas all other *t* tests resulted in $p < 0.05$, indicating that the values of HE, RE, and RC statistically differed for differently sized MNPs.

Modeling of the Size-Dependent Settling of Algae−Magnetic Nanoparticles Aggregates. To evaluate the size effect of MNPs on algal HE, we performed a modeling analysis for the settling velocity of MNP−algae aggregates in the magnetic field using the Stokes' law. We hypothesize that the settling velocity could depend on the sizes of MNPs that adsorbed onto the algae cells, and a higher settling velocity leads to a greater algal HE (e.g., a higher HE or RC). Details of the model development are provided in Supporting Information, Section S7. The mathematical relation of the settling velocity ($u_{\text{algae-MNPs}}$) and the MNPs radius (r_{MNPs}) under the influences of gravity, buoyancy force, drag force, and magnetic force is derived to

$$u_{\text{algae-MNPs}} = [8r_{\text{algae}}{}^{2}r_{\text{MNPs}}\rho_{\text{MNPs}}\left(g + M\frac{\partial B}{\partial x}\right) + 2\rho_{\text{algae}}r_{\text{algae}}{}^{3}g - 2\rho_{\text{medium}}(r_{\text{algae}} + 2r_{\text{MNPs}})^{3}g] / [9\eta(r_{\text{algae}} + 2r_{\text{MNPs}})] \quad (5)$$

where ρ_{algae}, ρ_{medium}, and ρ_{MNPs} are the densities for algae, water, and MNPs, respectively, g is the gravity constant, r_{algae} is the algae radius, η is the viscosity of water, $u_{\text{algae-MNPs}}$ is the settling velocity of the algae-MNPs aggregate (one algal cell with a number of MNPs adsorbed to), $\vec{M}$ is the magnetization of MNPs, $\vec{B}$ is the magnetic field strength (T), and x is the distance (cm) away from the magnet surface (Supporting Information, Figure S4 shows the magnetic field strength as a function of distance, x).

Figure 3 shows that the calculated settling velocity of MNP−algae aggregates greatly depends on the primary particle size of

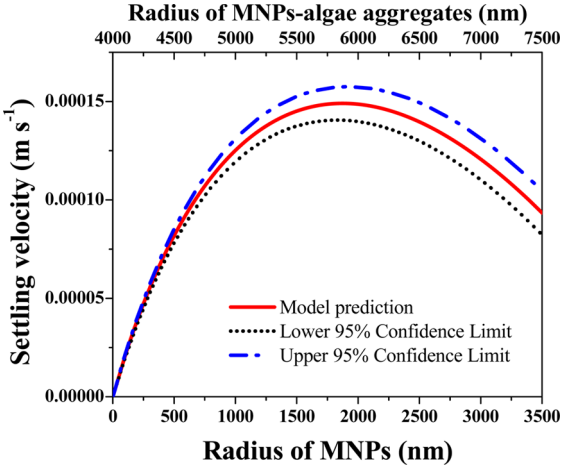

Figure 3. Relationship between settling velocity obtained from the physical model and the MNPs size.

MNPs. When the radius of MNPs is less than ~1900 nm, the settling velocity of algae−MNP aggregates increased as the size of MNPs increased. For MNPs with a radius greater than 1900 nm, the settling velocity declined, probably due to the decreased number of MNPs effectively adsorbed on algae (Supporting Information, Equation S18). A reduced settling velocity clearly corresponded to a lower algal HE, which explained the size dependence of HE, RE, or RC presented in

DOI: 10.1021/acsami.5b00572
ACS Appl. Mater. Interfaces 2015, 7, 6102−6108

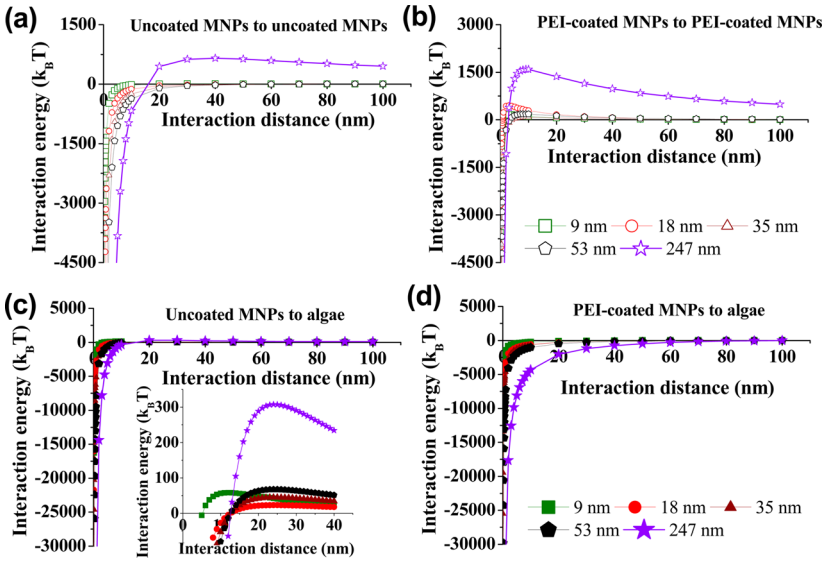

Figure 4. Total interaction energy as a function of the separation distance between different interacting entities: (a) uncoated MNPs-to-uncoated MNPs, (b) PEI-coated MNPs-to-PEI-coated MNPs, (c) uncoated MNPs-to-algae (inset shows the energy barriers), and (d) PEI-coated MNPs-to-algae. The legend of (b) was used in (a), and that of (d) was used in (c). The simulated interaction occurred in algal medium at pH = 7.0 ± 0.3 and the ionic strength of ~12.6 mM.

Figure 2b. However, one may notice that the HE began to decline at a diameter of 53 nm by TEM (179.7 nm by DLS), whereas the settling velocity declined at 1900 nm. This discrepancy might be attributed to the fact that we considered a monolayer of MNPs adsorbed on algae in our model (Supporting Information, Figure S2c), whereas MNPs may actually form multiple layers or aggregated clusters when they adsorbed to algae.

Interaction Energy between Algae and Magnetic Nanoparticles and Magnetic Nanoparticles Themselves with and without Polyethylenimine Coating. Magnetophoretic algal separation begins with surface adsorption, which is mediated by interfacial forces and interaction energy. Figure 4a shows that no energy barrier existed between uncoated MNPs (except 247 nm), while the interaction energy barriers between PEI-coated MNPs varied with particle size and reached up to 1600 k_BT (See Figure 4b), which indicates that PEI coating induced strong interparticle repulsion and therefore stabilized the dispersion of MNPs in water. On the contrary, uncoated MNPs could undergo rapid homoaggregation due to the strong interparticle attraction (negative interaction energy). Likewise, Figure 4c,d shows that the size of MNPs also affected the primary energy minima (large MNPs led to more negative interaction energy at the same distance). Energy barriers of ~21−290 k_BT existed between uncoated MNPs of different sizes and algae, whereas PEI-coated MNPs had no energy barrier (all negative interaction energy), suggesting that the adsorption of PEI-coated MNPs onto algae could be more thermodyanmically favorable than that of uncoated MNPs.[12]

Recovery and Reuse of Polyethylenimine-Coated Magnetic Nanoparticles. The concentrated MNP−algae aggregates were separated with the ultrasonic method as stated above. Figure 5 shows the recovery efficiencies for differently sized MNPs, which slightly varied with the particle size (see the *t*-test results in Supporting Information, Table S6). The highest recovery efficiency of 92.6% was achieved for 247 nm PEI-coated MNPs, whereas for 9 nm MNPs, the recovery efficiency

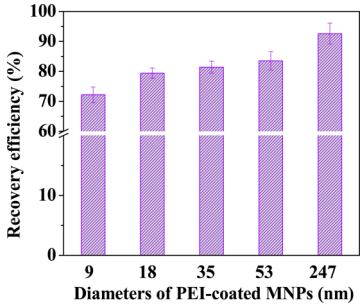

Figure 5. Recovery efficiency of five differently sized PEI-coated MNPs after detachment with *S. dimorphus*. The initial MNPs dose was 0.075 g·g^{-1} with the initial algal concentration of 0.8 g·L^{-1}. The magnetic field strength is 0.099 ± 0.009 T.

was 72%. The large-sized MNPs appeared to detach from algae relatively easily. Small MNPs are difficult to recover from algae biomass probably because they may have greater adhesion on the algal surface than larger ones did.[48] After the recovery, the PEI-coated MNPs may undergo the PEI coating again depending on the surface charge changes (PEI coating may be lost during the separation and rinse). The recovered MNPs were recoated with recycled PEI solution and reused for algal harvesting. Similar levels of HE, RE, and RC in algal harvesting were achieved (see details in Supporting Information, Figure S5 and elsewhere).[31]

Economic Implications. Of the numerous potential challenges in industrial-scale applications, economic viability of magnetophoretic algal separation is still the critical issue for the sustainability of algal biofuel.[7,9,14,46,49] This study shows that particle size significantly affects algal HE and the dose demand for MNPs. The rational design of MNPs should incorporate optimized particle sizes and surface coating (e.g., cationic polymers) to enhance the interactions of MNPs with algae, reduce the dose demand of MNPs, and enable the reuse of MNPs via cost-effective pathways.[4,6,7] The coating of iron oxide NPs (magnetite) with a polymer casing is often required to achieve desirable characteristics through multiple steps of

DOI: 10.1021/acsami.5b00572
ACS Appl. Mater. Interfaces 2015, 7, 6102−6108

manufacturing processes in large-scale production. Consequently, magnetic particles retail in the order of \$119 kg^{-1}, with some suppliers being dramatically more expensive. Taking the optimal dose (0.075 $g \cdot g^{-1}$) of MNPs, for example, there could be a direct cost of \$8.9 per cubic meter of algal suspension (assuming the algal concentration is 1 $g \cdot L^{-1}$) at laboratory scales. In fact, the cost of magnetophoretic algal separation could further be reduced to \$0.13−0.52 m^{-3} by reusing MNPs,[10] because ∼33% of this cost is mainly contributed by the cost of MNPs and the polymer binder. In comparison, energy consumption for filtration and flotation may range from 1 to 20 $kWh \cdot m^{-3}$ (\$0.11−2.2 m^{-3} if converted into dollar cost; Supporting Information, Table S7). Therefore, magnetophoretic algal separation may be more advantageous over other techniques, considering the simple operation and low maintenance.[50]

CONCLUSION

This study analyzed the effects of primary particle sizes of MNPs on algal HE. The present results, both modeling and experimental, suggest that the primary particle size of PEI-coated MNPs will significantly influence the settling process and the colloidal interactions between MNPs themselves and MNP−algae clusters. The settling velocity of MNP−algae aggregates increased with the increasing particle size but began to decline at large particle sizes, which coincided with the size dependence of HE, RE, and RC. Moreover, the recovery efficiency of MNPs from the harvested algae biomass also varied with the particle sizes. Overall, this study aims to provide fundamental evaluation of the size-dependent MNP−algae interactions and unravel the mechanisms of the size effects of MNPs on magnetophoretic algal harvesting, which is not only important for improving algal HE but also reduces the operational cost as well as the potential negative impacts on biolipid extraction from the harvested algal biomass.

ASSOCIATED CONTENT

Supporting Information

Reported algal recovery capacities, schematics of adsorption experiments, EDLVO equations, Hamaker constants, TEM, *t*-test results, mathematic modeling, algae harvesting performance, economic comparison of separation processes. This material is available free of charge via the Internet at http://pubs.acs.org.

AUTHOR INFORMATION

Corresponding Author

*E-mail: wzhang81@njit.edu. Phone: 1-973-596-5520. Fax: 1-973-596-5790.

Notes

The authors declare no competing financial interest.

ACKNOWLEDGMENTS

This study was partially supported by the Research Startup Fund at NJIT and National Science Foundation Grant No. CBET-1235166.

REFERENCES

(1) Coward, T.; Lee, J. G.; Caldwell, G. S. The Effect of Bubble Size on the Efficiency and Economics of Harvesting Microalgae by Foam Flotation. *J. Appl. Phycol.* **2014**, 1−10.

(2) Sharma, K. K.; Garg, S.; Li, Y.; Malekizadeh, A.; Schenk, P. M. Critical Analysis of Current Microalgae Dewatering Techniques. *Biofuels* **2013**, *4*, 397−407.

(3) Uduman, N.; Qi, Y.; Danquah, M. K.; Forde, G. M.; Hoadley, A. Dewatering of Microalgal Cultures: A major Bottleneck to Algae-based Fuels. *J. Renewable Sustainable Energy* **2010**, *2*, 012701−012707.

(4) Seo, J. Y.; Lee, K.; Lee, S. Y.; Jeon, S. G.; Na, J.-G.; Oh, Y.-K.; Park, S. B. Effect of Barium Ferrite Particle Size on Detachment Efficiency in Magnetophoretic Harvesting of Oleaginous *Chlorella sp.* *Bioresour. Technol.* **2014**, *152*, 562−566.

(5) Lim, J. K.; Chieh, D. C. J.; Jalak, S. A.; Toh, P. Y.; Yasin, N. H. M.; Ng, B. W.; Ahmad, A. L. Rapid Magnetophoretic Separation of Microalgae. *Small* **2012**, *8*, 1683−1692.

(6) Prochazkova, G.; Podolova, N.; Safarik, I.; Zachleder, V.; Branyik, T. Physicochemical Approach to Freshwater Microalgae Harvesting with Magnetic Particles. *Colloids Surf., B* **2013**, *112*, 213−218.

(7) Xu, L.; Guo, C.; Wang, F.; Zheng, S.; Liu, C.-Z. A Simple and Rapid Harvesting Method for Microalgae by in Situ Magnetic Separation. *Bioresour. Technol.* **2011**, *102*, 10047−10051.

(8) Zborowski, M.; Moore, L. R.; Williams, P. S.; Chalmers, J. J. Separations Based on Magnetophoretic Mobility. *Sep. Sci. Technol. (Philadelphia, PA, U. S.)* **2002**, *37*, 3611−3633.

(9) Hu, Y.-R.; Wang, F.; Wang, S.-K.; Liu, C.-Z.; Guo, C. Efficient Harvesting of Marine Microalgae *Nannochloropsis maritima* using Magnetic Nanoparticles. *Bioresour. Technol.* **2013**, *138*, 387−390.

(10) Toh, P. Y.; Yeap, S. P.; Kong, L. P.; Ng, B. W.; Chan, D. J. C.; Ahmad, A. L.; Lim, J. K. Magnetophoretic Removal of Microalgae from Fishpond Water: Feasibility of High Gradient and Low Gradient Magnetic Separation. *Chem. Eng. J. (Amsterdam, Neth.)* **2012**, *211−212*, 22−30.

(11) Yang, D.-Q.; Rochette, J.-F.; Sacher, E. Spectroscopic Evidence for $\pi-\pi$ Interaction between Poly (diallyl dimethylammonium) Chloride and Multiwalled Carbon Nanotubes. *J. Phys. Chem. B* **2005**, *109*, 4481−4484.

(12) Hu, Y.-R.; Guo, C.; Wang, F.; Wang, S.-K.; Pan, F.; Liu, C.-Z. Improvement of Microalgae Harvesting by Magnetic Nanocomposites Coated with Polyethylenimine. *Chem. Eng. J. (Amsterdam, Neth.)* **2014**, *242*, 341−347.

(13) Rashid, N.; Rehman, S. U.; Han, J.-I. Rapid Harvesting of Freshwater Microalgae using Chitosan. *Process Biochem. (Oxford, U. K.)* **2013**, *48*, 1107−1110.

(14) Lee, Y.; Lee, K.; Hwang, Y.; Andersen, H. R.; Kim, B.; Lee, S. Y.; Choi, M.; Park, J.; Han, Y.; Oh, Y.; Huh, Y. S. Aminoclay-templated Nanoscale Zero-valent Iron (nZVI) Synthesis for Efficient Harvesting of Oleaginous Microalga, *Chlorella* sp. KR-1. *RSC Adv.* **2014**, *4*, 4122−4127.

(15) Van Oss, C. J. *Interfacial Forces in Aqueous Media;* CRC Press: Boca Ration, FL, 2006.

(16) Toh, P. Y.; Ng, B. W.; Ahmad, A. L.; Chieh, D. C. J.; Lim, J. The Role of Particle-to-cell Interactions in Dictating Nanoparticle Aided Magnetophoretic Separation of Microalgal Cells. *Nanoscale* **2014**, *6*, 12838−12848.

(17) Quigg, A.; Chin, W.-C.; Chen, C.-S.; Zhang, S.; Jiang, Y.; Miao, A.-J.; Schwehr, K. A.; Xu, C.; Santschi, P. H. Direct and Indirect Toxic Effects of Engineered Nanoparticles on Algae: Role of Natural Organic Matter. *ACS Sustainable Chem. Eng.* **2013**, *1*, 686−702.

(18) Zhang, W.; Zhang, X. Adsorption of MS2 on Oxide Nanoparticles Affects Chlorine Disinfection and Solar Inactivation. *Water Res.* **2015**, *69*, 59−67.

(19) Miao, A.; Zhang, X.; Luo, Z.; Chen, C.; Chin, W.; Santschi, P. H.; Quigg, A. Zinc Oxide-engineered Nanoparticles: Dissolution and Toxicity to Marine Phytoplankton. *Environ. Toxicol. Chem.* **2010**, *29*, 2814−2822.

(20) Miao, A. J.; Schwehr, K. A.; Xu, C.; Zhang, S. J.; Luo, Z.; Quigg, A.; Santschi, P. H. The Algal Toxicity of Silver Engineered Nanoparticles and Detoxification by Exopolymeric Substances. *Environ. Pollut. (Oxford, U. K.)* **2009**, *157*, 3034−41.

DOI: 10.1021/acsami.5b00572
ACS Appl. Mater. Interfaces 2015, 7, 6102−6108

(21) Hund-Rinke, K.; Simon, M. Ecotoxic Effect of Photocatalytic Active Nanoparticles (TiO_2) on Algae and Daphnids. *Environ. Sci. Pollut. Res.* **2006**, *13*, 225−232.
(22) Zhang, W.; Rittmann, B.; Chen, Y. Size Effects on Adsorption of Hematite Nanoparticles on *E. Coli* Cells. *Environ. Sci. Technol.* **2011**, *45*, 2172−8.
(23) Sun, J.; Zhou, S.; Hou, P.; Yang, Y.; Weng, J.; Li, X.; Li, M. Synthesis and Characterization of Biocompatible Fe_3O_4 Nanoparticles. *J. Biomed. Mater. Res., Part A* **2007**, *80*, 333−341.
(24) Roca, A. G.; Marco, J. F.; Morales, M. d. P.; Serna, C. J. Effect of Nature and Particle Size on Properties of Uniform Magnetite and Maghemite Nanoparticles. *J. Phys. Chem. C* **2007**, *111*, 18577−18584.
(25) Park, J.; An, K.; Hwang, Y.; Park, J.-G.; Noh, H.-J.; Kim, J.-Y.; Park, J.-H.; Hwang, N.-M.; Hyeon, T. Ultra-large-scale Syntheses of Monodisperse Nanocrystals. *Nat. Mater.* **2004**, *3*, 891−895.
(26) Fulton, L. M. *Nutrient Removal by Algae Grown in CO_2-Enriched Wastewater over a Range of Nitrogen-to-Phosphorus Ratios*. MS Thesis, California Polytechnic State University, November 2009.
(27) Su, Y.; Mennerich, A.; Urban, B. Coupled Nutrient Removal and Biomass Production with Mixed Algal Culture: Impact of Biotic and Abiotic Factors. *Bioresour. Technol.* **2012**, *118*, 469−476.
(28) Agbakpe, M.; Ge, S.; Zhang, W.; Zhang, X.; Kobylarz, P. Algae Harvesting for Biofuel Production: Influences of UV Irradiation and Polyethylenimine (PEI) Coating on Bacterial Biocoagulation. *Bioresour. Technol.* **2014**, *166*, 266−272.
(29) Kumar, S.; Yang, H.; Zou, S. Seed-Mediated Growth of Uniform Gold Nanoparticle Arrays. *J. Phys. Chem. C* **2007**, *111*, 12933−12938.
(30) Li, Z.; Kawashita, M.; Araki, N.; Mitsumori, M.; Hiraoka, M.; Doi, M. Magnetite Nanoparticles with High Heating Efficiencies for Application in the Hyperthermia of Cancer. *Mater. Sci. Eng., C* **2010**, *30*, 990−996.
(31) Ge, S.; Agbakpe, M.; Wu, Z.; Kuang, L.; Zhang, W.; Wang, X. Influences of Surface Coating, UV Irradiation and Magnetic Field on the Algae Removal using Magnetite Nanoparticles. *Environ. Sci. Technol.* **2015**, *49*, 1190−1196.
(32) Salim, S.; Bosma, R.; Vermuë, M.; Wijffels, R. Harvesting of Microalgae by Bio-flocculation. *J. Appl. Phycol.* **2011**, *23*, 849−855.
(33) Boström, M.; Deniz, V.; Franks, G. V.; Ninham, B. W. Extended DLVO Theory: Electrostatic and Non-electrostatic Forces in Oxide Suspensions. *Adv. Colloid Interface Sci.* **2006**, *123*−*126*, 5−15.
(34) Hoek, E.; Agarwal, G. K. Extended DLVO Interactions between Spherical Particles and Rough Surfaces. *J. Colloid Interface Sci.* **2006**, *298*, 50−58.
(35) Zhang, Q. *Synthesis and Characterization of Novel Magnetite Nanoparticle Block Copolymer Complexes*. Ph.D. Dissertation, Virginia Polytechnic Institute and State University, April 2007.
(36) Runkana, V.; Somasundaran, P.; Kapur, P. C. A Population Balance Model for Flocculation of Colloidal Suspensions by Polymer Bridging. *Chem. Eng. Sci.* **2006**, *61*, 182−191.
(37) Toh, P. Y.; Ng, B. W.; Ahmad, A. L.; Chieh, D. C. J.; Lim, J. Magnetophoretic Separation of *Chlorella* sp.: Role of Cationic Polymer Binder. *Process Saf. Environ. Prot.* **2014**, *92*, 515−521.
(38) Yeap, S. P.; Toh, P. Y.; Ahmad, A. L.; Low, S. C.; Majetich, S. A.; Lim, J. Colloidal Stability and Magnetophoresis of Gold-coated Iron Oxide Nanorods in Biological Media. *J. Phys. Chem. C* **2012**, *116*, 22561−22569.
(39) Zhang, W.; Crittenden, J.; Li, K.; Chen, Y. Attachment Efficiency of Nanoparticle Aggregation in Aqueous Dispersions: Modeling and Experimental Validation. *Environ. Sci. Technol.* **2012**, *46*, 7054−7062.
(40) Li, K.; Zhang, W.; Huang, Y.; Chen, Y. Aggregation Kinetics of CeO_2 Nanoparticles in KCl and $CaCl_2$ Solutions: Measurements and Modeling. *J. Nanopart. Res.* **2011**, *13*, 6483−6491.
(41) Li, K.; Chen, Y. Effect of Natural Organic Matter on the Aggregation Kinetics of CeO_2 Nanoparticles in KCl and $CaCl_2$ Solutions: Measurements and Modeling. *J. Hazard. Mater.* **2012**, *209*−*210*, 264−270.
(42) Zhang, W.; Yao, Y.; Li, K.; Huang, Y.; Chen, Y. Influence of Dissolved Oxygen on Aggregation Kinetics of Citrate-coated Silver Nanoparticles. *Environ. Pollut. (Oxford, U. K.)* **2011**, *159*, 3757−3762.
(43) Zhang, W.; Yao, Y.; Sullivan, N.; Chen, Y. Modeling the Primary Size Effects of Citrate-Coated Silver Nanoparticles on Their Ion Release Kinetics. *Environ. Sci. Technol.* **2011**, *45*, 4422−4428.
(44) Zaitsev, V. S.; Filimonov, D.; Presnyakov, I. A.; Gambino, R. J.; Chu, B. Physical and Chemical Properties of Magnetite and Magnetite-Polymer Nanoparticles and Their Colloidal Dispersions. *J. Colloid Interface Sci.* **1999**, *212*, 49−58.
(45) Gutierrez, L.; Mylon, S. E.; Nash, B.; Nguyen, T. H. Deposition and Aggregation Kinetics of Rotavirus in Divalent Cation Solutions. *Environ. Sci. Technol.* **2010**, *44*, 4552−4557.
(46) Prochazkova, G.; Safarik, I.; Branyik, T. Harvesting Microalgae with Microwave Synthesized Magnetic Microparticles. *Bioresour. Technol.* **2013**, *130*, 472−477.
(47) Cerff, M.; Morweiser, M.; Dillschneider, R.; Michel, A.; Menzel, K.; Posten, C. Harvesting Fresh Water and Marine Algae by Magnetic Separation: Screening of Separation Parameters and High Gradient Magnetic Filtration. *Bioresour. Technol.* **2012**, *118*, 289−295.
(48) Zhang, W.; Stack, A. G.; Chen, Y. Interaction Force Measurement between *E. coli* Cells and Nanoparticles Immobilized Surfaces by using AFM. *Colloids Surf., B* **2011**, *82*, 316−324.
(49) Lee, Y.-C.; Lee, H. U.; Lee, K.; Kim, B.; Lee, S. Y.; Choi, M.-H.; Farooq, W.; Choi, J. S.; Park, J.-Y.; Lee, J.; Oh, Y.-K.; Huh, Y. S. Aminoclay-conjugated TiO_2 Synthesis for Simultaneous Harvesting and Wet-disruption of Oleaginous *Chlorella sp. Chem. Eng. J. (Amsterdam, Neth.)* **2014**, *245*, 143−149.
(50) Hoffmann, C.; Franzreb, M.; Holl, W. A Novel High-Gradient Magnetic Separator (HGMS) Design for Biotech Applications. *IEEE Trans. Appl. Supercond.* **2002**, *12*, 963−966.

DOI: 10.1021/acsami.5b00572
ACS Appl. Mater. Interfaces 2015, 7, 6102−6108